Cell

The Structure of the ζζ Transmembrane Dimer Reveals Features Essential for Its Assembly with the T Cell Receptor

Matthew E. Call,[1,2,4] Jason R. Schnell,[3,4] Chenqi Xu,[1] Regina A. Lutz,[1] James J. Chou,[3,*] and Kai W. Wucherpfennig[1,2,*]
[1] Department of Cancer Immunology and AIDS, Dana-Farber Cancer Institute
[2] Program in Immunology
[3] Department of Biological Chemistry and Molecular Pharmacology
Harvard Medical School, Boston, MA 02115, USA
[4] These authors contributed equally to this study.
*Contact: james_chou@hms.harvard.edu (J.J.C.), kai_wucherpfennig@dfci.harvard.edu (K.W.W.)
DOI 10.1016/j.cell.2006.08.044

SUMMARY

The T cell receptor (TCR) αβ heterodimer communicates ligand binding to the cell interior via noncovalently associated CD3γε, CD3δε, and ζζ dimers. While structures of extracellular components of the TCR-CD3 complex are known, the transmembrane (TM) domains that mediate assembly have eluded structural characterization. Incorporation of the ζζ signaling module is known to require one basic TCRα and two ζζ aspartic acid TM residues. We report the NMR structure of the $\zeta\zeta_{TM}$ dimer, a left-handed coiled coil with substantial polar contacts. Mutagenesis experiments demonstrate that three polar positions are critical for ζζ dimerization and assembly with TCR. The two aspartic acids create a single structural unit at the ζζ interface stabilized by extensive hydrogen bonding, and there is evidence for a structural water molecule (or molecules) within close proximity. This structural unit, representing only the second transmembrane dimer interface solved to date, serves as a paradigm for the assembly of all modules involved in TCR signaling.

INTRODUCTION

The T cell receptor (TCR) recognizes peptide fragments presented by MHC molecules and delivers signals that control T cell development and function. The TCRαβ heterodimer communicates ligand binding events to the interior of the cell via the noncovalently associated CD3γε, CD3δε, and ζζ dimers that contain tyrosine-based phosphorylation motifs (Samelson et al., 1985; Sussman et al., 1988; Weissman et al., 1988; Exley et al., 1991). Early studies suggested that basic and acidic residues in the transmembrane (TM) domains of the TCR and CD3 subunits contribute to assembly (Alcover et al., 1990; Blumberg et al., 1990; Rutledge et al., 1992; Dietrich et al., 1996), and it was proposed that these residues form pairwise interactions similar to salt bridges (Cosson et al., 1991). There are three basic residues in the TM domains of the TCRαβ heterodimer and a pair of acidic residues in the TM regions of each of the three dimeric signaling modules, and we recently demonstrated that each of three assembly steps requires the formation of a three-chain interface involving a basic TCR TM residue and both acidic TM residues of the respective signaling dimer (Call et al., 2002). Formation of the eight-chain TCRαβ-CD3δε-CD3γε-ζζ complex is thus dependent on proper placement of three groups of three ionizable TM residues (Punt et al., 1994; Kearse et al., 1995; Call et al., 2002, 2004).

Subsequent studies demonstrated that a diverse group of activating receptors in cells of hematopoietic origin converged on a strikingly similar assembly mechanism involving basic and acidic TM residues (Feng et al., 2005; Garrity et al., 2005). Examples include the natural killer (NK) cell receptors KIR2DS, NKp46, and NKG2C/CD94; the FcαRI receptor for IgA; and the platelet collagen receptor GPVI (Feng et al., 2005; Lanier, 2005). Each of these receptors assembles with a signaling module belonging to one of two major families: the ζ chain and the common Fc receptor γ subunit (Fcγ) form one family (Samelson et al., 1985; Sussman et al., 1988; Kuster et al., 1990), while the DAP10 and DAP12 proteins form the second (Tomasello et al., 1998; Lanier et al., 1998a; Wu et al., 1999). The ζ chain and Fcγ share a high degree of sequence homology within the TM domains and have conserved cysteine and aspartic acid residues at positions 2 and 6 of the predicted TM domains, respectively. In the DAP10 and DAP12 dimers, the aspartic acid pair is located closer to the center of the TM domains, and the interchain disulfide bonds are positioned in the short ectodomains.

Surprisingly, TM peptides are sufficient for assembly of several distinct receptors with their signaling modules.

For example, a TCRα TM peptide assembles with CD3δε (Call et al., 2002), and TM peptides of the KIR and NKG2C receptors each form the appropriate three-chain complex with the DAP12 signaling module (Feng et al., 2005). A major unresolved question concerns how the two acidic TM residues of the dimeric signaling modules create the essential functional unit for assembly of these diverse receptor complexes. Biochemical studies suggest that the two acidic TM residues act as a functional pair because mutation of aspartic acid to asparagine (N) or alanine (A) in even one strand results in profound assembly defects (Call et al., 2002; Feng et al., 2005; Garrity et al., 2005). Given this striking result, a central goal is to understand how the orientation and ionization states of the two acidic side chains relate to the formation of the critical structure for receptor assembly. These findings therefore raise the following critical questions: Are the two aspartic acids within sufficient proximity to interact directly with each other? If that is the case, how is such an interaction between two highly polar acidic groups stabilized in the membrane? To directly address these issues, we determined the structure of the ζ chain TM ($\zeta\zeta_{TM}$) dimer as a representative signaling module through multidimensional solution NMR methods. The disulfide-stabilized ζζ dimer specifically interacts with the TM arginine of the TCRα chain and also acts as the signaling subunit for the activating NK cell receptor NKp46 (Vitale et al., 1998). Given the high degree of sequence homology between ζ and Fcγ, the structure of the $\zeta\zeta_{TM}$ dimer is also relevant for receptors that associate with the Fcγ dimer, such as the Fc receptor for IgA, the platelet collagen receptor GPVI, and the osteoclast receptor OSCAR (Ishikawa et al., 2004; Feng et al., 2005).

The technical challenges in expression, reconstitution, and structural NMR analysis of a hydrophobic peptide dimer are substantial, and only one such structure has been reported to date. Pioneering work on the erythrocyte surface protein glycophorin A (GpA) demonstrated that interactions among the TM domains result in a highly stable dimer. Mutagenesis studies identified a 7 residue TM dimerization motif (LIxxGVxxGVxxT) (Lemmon et al., 1992a, 1992b), and the solution NMR structure of the GpA TM dimer demonstrated intimate contacts between the two TM helices involving the two critical glycines of one strand and opposing valines of the other strand (MacKenzie et al., 1997). It has been postulated that a similar glycine-based motif directs $\zeta\zeta_{TM}$ dimerization (Bolliger and Johansson, 1999), but we report that the $\zeta\zeta_{TM}$ dimer is in fact different from GpA in almost every aspect, displaying polar features that are critical for both ζζ dimer formation and functional association with the TCR-CD3 complex.

RESULTS

Production and Reconstitution of $\zeta\zeta_{TM}$ Peptide Dimer for NMR Studies

We expressed a 33 amino acid peptide with the sequence DSKLCYLLDGILFIYGVILTALFLRVKFSRSAD, corresponding to the predicted ζ_{TM} region (underlined), with 3 N-terminal and 7 C-terminal residues of native flanking sequence. This ζ_{TM} peptide was expressed as a fusion to the C terminus of the trpLE sequence (Staley and Kim, 1994), with a methionine residue N-terminal to the ζ sequence for removal of trpLE by cyanogen bromide (CNBr) cleavage. A single substitution (proline to serine) at position −2 relative to the TM sequence was introduced to avoid secondary cleavage at aspartate/proline. This mutation had no effect on ζζ dimer formation (data not shown). Expression of the trpLE-ζ_{TM} fusion protein was highly sensitive to culture conditions, and sufficient yield was only observed under conditions that slowed the synthesis of the fusion, including growth at low temperature (20°C) in minimal medium and low IPTG concentration (0.125 mM; see Figure 1A). Further optimization (see Experimental Procedures) resulted in a maximum yield of 50 mg/l for ^{15}N- and ^{15}N-, ^{13}C-labeled proteins.

The ζ chain assembles with the TCR-CD3 complex as a covalent homodimer that is disulfide linked through a cysteine at position two of the predicted TM region (Sussman et al., 1988; Geisler et al., 1989; Rutledge et al., 1992; Call et al., 2002). We therefore developed a strategy to assemble, purify, and reconstitute dimeric $\zeta\zeta_{TM}$ peptide in detergent micelles for solution NMR (Figure 1B). The trpLE-ζ_{TM} fusion was extracted from inclusion bodies in guanidine HCl with 1% Triton X-100 and bound to a Ni-NTA column through an N-terminal His tag. After extensive washing, the fusion protein was disulfide crosslinked on the column with an oxidizing urea solution. The $\zeta\zeta_{TM}$ dimer was purified from a CNBr digest by reverse-phase HPLC (RP-HPLC) on a C4 column (Figure 1C).

For NMR structure determination, we attempted to reconstitute ^{15}N-labeled $\zeta\zeta_{TM}$ dimer in a variety of detergent and lipid systems and evaluated the conditions by 2D ^{1}H-^{15}N heteronuclear single-quantum coherence (HSQC) spectroscopy. We initially found that the peptide dimer was only partially soluble or produced poor spectra in several different detergents. Because TM peptides can assume α-helical secondary structure in sodium dodecyl sulfate (SDS; Popot et al., 1987), we also evaluated a mixed detergent system of SDS and dodecyl phosphocholine (DPC). Reconstitution of $\zeta\zeta_{TM}$ in 20 mM SDS at pH 7.0 yielded an excellent HSQC spectrum, and we then titrated in the milder DPC. Initial additions caused large changes in the spectrum, as measured by the average change in the backbone ^{15}N-^{1}H chemical shift (Figure 1D). However, with >3:1 molar excess of DPC, little additional change in the spectrum was observed. Ratios between 4.8:1 and 8.4:1 showed no significant differences, indicating that the chemical environment of the peptide dimer was stable over this range. DPC:SDS ratios of 10:1 or higher resulted in aggregation, indicating that some SDS was indeed required. We therefore performed all subsequent NMR experiments at a 5:1 DPC:SDS ratio (see Figure 2A). A large body of functional data demonstrate that the structure is relevant for the native ζζ dimer, as described in detail below.

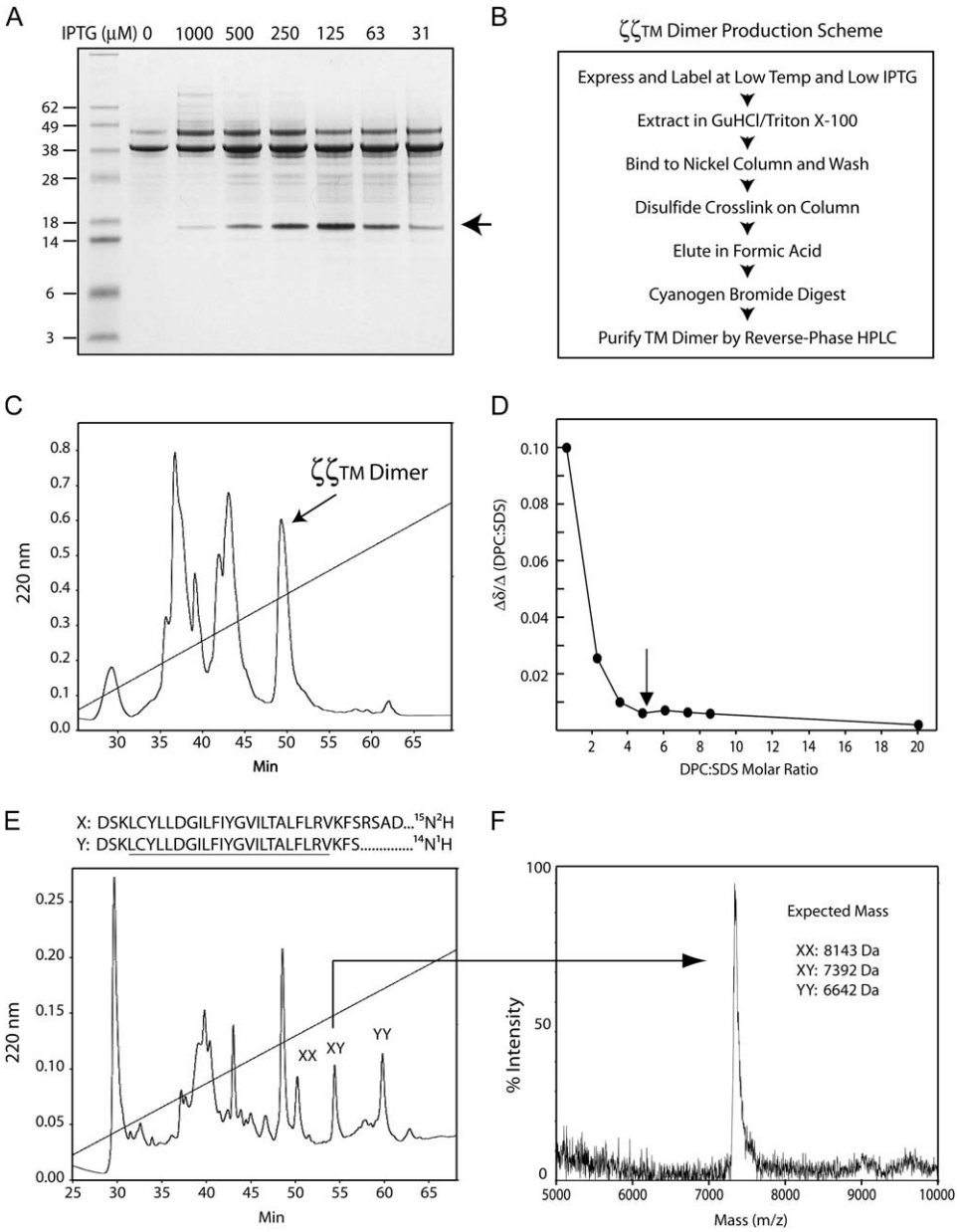

Figure 1. Production of Stable-Isotope-Labeled $\zeta\zeta_{TM}$ Peptide Dimers for NMR Studies

(A) Expression required culture conditions that slowed down production of the hydrophobic trpLE-ζ_{TM} fusion protein. Even at a low temperature (20°C), production of the trpLE-ζ_{TM} fusion protein (arrow) in BL21(DE3) cells required low concentrations of IPTG for induction of expression.

(B) Flow chart for production of $\zeta\zeta_{TM}$ dimer.

(C) Reverse-phase HPLC (RP-HPLC) purification of $\zeta\zeta_{TM}$ dimer from cyanogen-bromide-cleaved trpLE-ζ_{TM} on a C4 column with a gradient from 40% to 95% acetonitrile, 0.1% TFA.

(D) ^{15}N-labeled $\zeta\zeta_{TM}$ dimer was initially prepared in 20 mM SDS. DPC was subsequently titrated into the sample, and HSQC spectra were recorded at different DPC:SDS ratios. A plot is shown of the observed changes in chemical shift of backbone ^{15}N-^{1}H correlations averaged for the entire 23 residue core TM domain ($\Delta\delta$) in relationship to the DPC:SDS molar ratios tested. Arrow (5:1 ratio of DPC:SDS) indicates the conditions chosen for subsequent analysis.

(E) A mixed-label $\zeta\zeta_{TM}$ dimer sample was produced for definition of the $\zeta\zeta_{TM}$ dimer interface by nuclear Overhauser effect spectroscopy (NOESY). Two trpLE-ζ_{TM} fusion proteins that differed in the length of the ζ cytoplasmic segment were expressed: One ζ_{TM} peptide was uniformly ^{15}N ^{2}H-labeled (designated strand X), while the other was unlabeled (^{14}N ^{1}H, designated strand Y). The two cultures were mixed and processed as outlined in (B), and the three different covalent $\zeta\zeta_{TM}$ dimers (XX, XY, and YY) were separated by RP-HPLC based on the higher degree of hydrophobicity of strand Y.

(F) The identity of the desired product (XY) was verified by mass spectrometry.

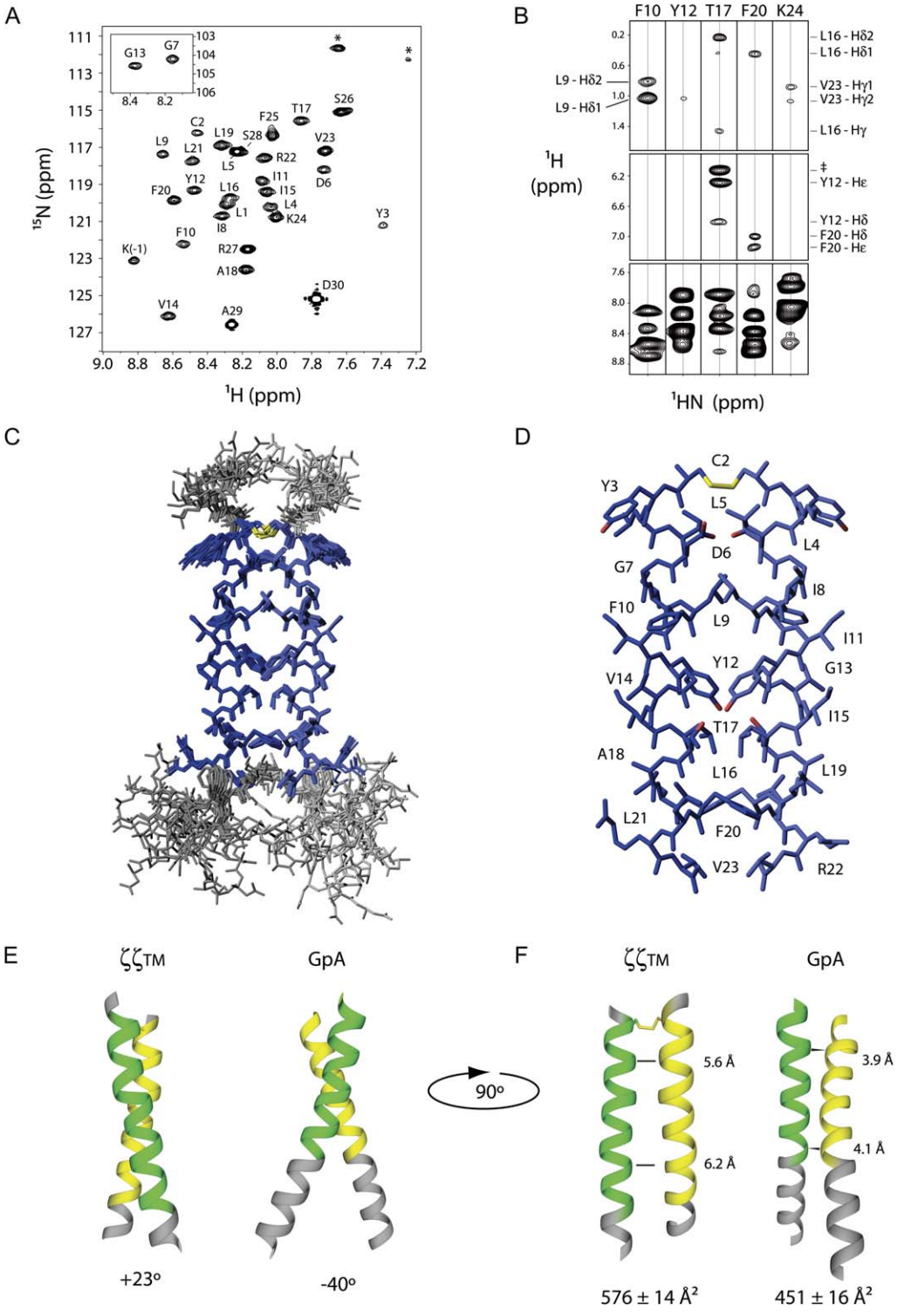

Figure 2. Solution Structure of the $\zeta\zeta_{TM}$ Dimer

(A) An ^{15}N-^{1}H HSQC spectrum of $\zeta\zeta_{TM}$ in 5:1 DPC:SDS micelles. Residue assignments for backbone amides are shown. Glycine region is shown as inset. * indicates the side-chain NH_{ε} of arginine.

(B) Selected strips of a ^{15}N-edited NOESY spectrum of a mixed-label (^{15}N ^{2}H and unlabeled) $\zeta\zeta_{TM}$ dimer showing interchain NOEs. The methyl (top), aromatic (middle), and amide (bottom) regions are shown for residues that have large NOEs to interface residues of the opposing helix. The lack of intrachain NOEs in the Y12 strip demonstrates the completeness of labeling. ‡ indicates a hydroxyl proton from the hydrogen bonding network between Y12 and T17.

Structure determination by NMR required measurement of nuclear Overhauser effects (NOEs) across the dimer interface, but interchain NOEs cannot be distinguished from intrachain NOEs in a uniformly labeled dimer. We therefore developed a strategy to produce a dimer in which one strand was ^{15}N-labeled and fully deuterated (Figure 1E, strand X) while the other strand was unlabeled (strand Y) to allow unambiguous assignment of interchain NOEs (Walters et al., 1997). Cultures expressing either ^{15}N ^{2}H-labeled trpLE-ζ_{TM} (produced in D_2O with deuterated glucose) or an unlabeled form shortened by 4 residues at the C terminus were grown separately and combined for purification as outlined in Figure 1B. The three different disulfide-linked dimers (XX, XY, and YY) were well separated by RP-HPLC due to the higher hydrophobicity of the shorter Y strand (see Figure 1E), and the pure mixed dimer (XY) was unambiguously identified by mass spectrometry (Figure 1F).

Solution NMR Structure of the $\zeta\zeta_{TM}$ Dimer

The solution structure was determined exclusively by NMR measurements, without the use of any knowledge-based structural constraints. An ensemble of 15 structures (rms difference of 0.31 Å and 0.65 Å for backbone and all heavy atoms, respectively) was calculated from an extensive experimental data set, including 426 intrahelical and 46 interhelical NOE-derived distances, 70 global orientation restraints from residual dipolar couplings (RDCs), and 42 side-chain dihedral angles from three-bond *J* couplings (Table 1). We emphasize that accurate determination of side-chain conformation is crucial for analysis of TM helix packing, as previously shown for the GpA TM dimer (MacKenzie et al., 1996) and the pentameric phospholamban (Oxenoid and Chou, 2005).

The structure of the GpA TM dimer is an instructive model for helix-helix interactions within the lipid bilayer (MacKenzie et al., 1997). Interestingly, the $\zeta\zeta_{TM}$ dimer adopts a strikingly different conformation (Figures 2C–2F). The GpA dimer is a right-handed coiled coil with a crossing angle of −40°, whereas $\zeta\zeta_{TM}$ forms a left-handed coiled coil crossing at a much less severe +23° angle (Figure 2E). The portion of the $\zeta\zeta_{TM}$ making interchain contacts (colored yellow and green) comprises almost the entire TM domain (20 of 23 TM residues), while close contacts in the GpA dimer are restricted to a shorter segment (13 of 23 TM residues). This translates to ~30% more buried surface area in the $\zeta\zeta_{TM}$ dimer interface (576 Å versus 451 Å for GpA; Figure 2F). However, the interstrand distance is considerably smaller in GpA compared to the $\zeta\zeta_{TM}$ dimer (Figure 2F), reflecting the predominance of small side-chain packing and backbone-backbone contacts in the GpA interface, while the $\zeta\zeta_{TM}$ dimer interface is composed almost entirely of side-chain contacts, several of which are polar.

Table 1. NMR Structural Statistics and Atomic Rms Differences

Quantity	Number of Restraints	Violations per Structure
NOEs	236	0 (>0.1 Å)
Intramolecular	213	0
Intermolecular	23	0
Dihedral angle restraints	21	0 (>5°)
χ_1	16	0
χ_2	5	0
Dipolar coupling restraints (Hz)[a]	35	2.69 ± 0.23
NH	21	1.84 ± 0.08
$C^{\alpha}H^{\alpha}$	14	3.74 ± 0.44
Deviations from idealized covalent geometry		
Bonds (Å)	0.0019 ± 0.0001	
Angles (°)	0.21 ± 0.01	
Impropers (°)	0.19 ± 0.03	
Coordinate precision (Å)[b]		
All heavy atoms	0.65	
Backbone heavy atoms	0.31	
Ramachandran plot statistics (%)[c]		
Most favored regions	100	

Statistics are calculated and averaged over an ensemble of the 15 lowest energy structures. The number of experimental restraints given is per monomer.

[a] Violations are given as the rms difference (in Hz) between individual sets of experimental dipolar couplings and those predicted by the 15 final structures by means of SVD fit. The $^{1}D_{C\alpha H\alpha}$ couplings are normalized to $^{1}D_{NH}$.

[b] The precision of the atomic coordinates is defined as the average rms difference between the 15 final structures and their mean coordinates. Unstructured residues at the N terminus (DSK-) and C terminus (-SRSAD) were excluded.

[c] As evaluated for the structured region (residues 1–25) with the program PROCHECK (Laskowski et al., 1993).

(C) Representative ensemble of 15 $\zeta\zeta_{TM}$ structures calculated using simulated annealing and chosen based on lowest overall energy. The highly structured region (residues 2–23) is colored blue, and flanking regions are colored gray. The C2 disulfide bond is shown in yellow.

(D) Representative structure from the ensemble showing the structured region (residues 2–23) with residue labels. Side-chain oxygens and the disulfide-bond sulfurs are shown in red and yellow, respectively.

(E and F) Comparison of the packing modes of $\zeta\zeta_{TM}$ and GpA. The helical regions of $\zeta\zeta_{TM}$ and GpA are shown as ribbon diagrams with regions of close intermolecular contact colored green/yellow. Residues with close interchain contact were defined as having any heavy backbone atom within 7 Å of any other heavy backbone atom from the opposing helix. The handedness and angle of packing is illustrated in (E). In (F), the diagrams have been rotated by 90° to illustrate the extent and closeness of interchain packing. Representative backbone-backbone distances are shown along the interface, and average buried surface area is shown below.

Polar and Nonpolar Side-Chain Contacts Contribute to $\zeta\zeta_{TM}$ Dimer Formation

The $\zeta\zeta_{TM}$ dimer interface is defined by interstrand contacts involving a total of 8 residues (red in Figure 3A). To test the functional importance of these contacts, we made substitutions of interface and noninterface residues in the full-length human ζ chain sequence and evaluated their effects on covalent ζζ dimer formation (Figures 3B–3E). Analysis of these mutants was performed using an in vitro translation system with ER microsomes with which we previously characterized the TM interactions directing the assembly of the TCR-CD3 complex and other activating immune receptors (Call et al., 2002; Feng et al., 2005; Garrity et al., 2005). In these experiments, mRNAs encoding a WT or mutant ζ chain sequence (or sequences) were cotranslationally translocated into purified ER microsomes and allowed to fold and assemble under redox conditions similar to those found in cells. The ER-associated proteins were then analyzed by SDS-PAGE to assess the degree of disulfide-linked dimer formation. Consistent with the $\zeta\zeta_{TM}$ dimer structure, substitutions at positions D6, L9, Y12, T17, and F20 (Figures 3B and 3C) resulted in impaired dimer formation, while mutation of the noninterface residues Y3, F10, and R22 had little effect. Interestingly, mutation of Y12 and T17 had the most dramatic effect on dimerization (14% and 24% compared to WT, respectively). Each Y12-T17 pair makes an interchain hydrogen bond that is critical for dimer assembly, as discussed in more detail below (Figure 4). Surprisingly, mutation of L16 had little effect on dimerization despite its position at the interface. This may be explained by the observation that the L16-L16 contact is "bracketed" by the Y12-T17 hydrogen bonds on both sides (see Figure 4 and below). G13 has been proposed to represent a key interface contact based on a GpA-derived model of the ζζ dimer (Bolliger and Johansson, 1999). While G13 is in the dimer interface, the Cα-to-Cα distance at this residue is ~5.5 Å, and substitution of G13 by alanine is well tolerated (Figure 3B, lane 6). G13 thus does not make a direct contribution to $\zeta\zeta_{TM}$ dimer stability.

It has previously been shown that the aspartic acid at position 6 in the $\zeta\zeta_{TM}$ region plays an important role in dimerization (Rutledge et al., 1992; Call et al., 2002), and the $\zeta\zeta_{TM}$ dimer structure demonstrates that the two aspartic acids pack closely within the interface. Further functional analysis revealed that an acidic residue (D or E) was required for dimerization at WT levels (Figure 3C, lanes 1 and 2) and that substitution of D6 by other polar residues (N or S, lanes 3 and 4) reduced the level of dimer formation to 40%–45%. Efficient dimerization was observed for mixed dimers of one WT and one mutant chain with a different polar residue (E, N, or S) at position 6 (Figure 3D, lanes 2–4), and only the mixed dimer between a WT and a D6A mutant chain showed impaired dimer formation (lane 5). A kinetic analysis of this D-A combination (Figure 3E) indicated that while the D-A mixed dimer accumulated to 60% of WT by 60 min, the initial rate of dimer formation was reduced 8- to 10-fold compared to WT. These results demonstrate that both aspartic acids participate in ζζ dimer formation and that other polar residues only partially support dimerization.

Both Lateral Y12-T17 Hydrogen Bonds Are Required for $\zeta\zeta_{TM}$ Dimerization

The hydroxyl groups of Y12 and T17 in one strand form hydrogen bonds with the hydroxyl groups of T17 and Y12 in the opposite strand, respectively (Figures 4A and 4B). These two contacts form "brackets" that create the lateral edges of the dimer interface. As shown in Figure 4B, the T17 hydroxyl is simultaneously hydrogen bonded to the Y12 hydroxyl from the opposite strand and to the backbone carbonyl oxygen of the *i*-4 residue of the same strand. Side-chain packing did not appear to play a major role at this position per se because even the Y12F mutation substantially reduced dimerization (Figure 4C, lane 3). Furthermore, the initial rate of T17A dimer formation was found to be 25-fold lower than WT even though the disulfide-bonded dimer accumulated to 30% of WT by 60 min (Figure 4E).

Importantly, both Y12-T17 hydrogen bonds were required because a single mutation in only one chain reduced dimerization to 16%–25% of WT (Figure 4D, bold red type). Even removal of a single hydroxyl group from one strand of the dimer (Y12F, Figure 4D, lane 3) substantially reduced dimer formation. The Y12-T17 hydrogen bonds therefore constitute a critical feature of the dimer interface. These functional data also confirm that the NMR structure is relevant to the native ζζ dimer, even though the protein was expressed in *E. coli* and reconstituted in a mixed detergent micelle system.

Structural Features of the ζζ Dimer Relevant for Assembly with the TCR-CD3 Complex

Mutations that disrupt dimerization, most notably at residues D6, Y12, and T17, prevent formation of the native disulfide bond through C2. What, then, is the role of C2 in dimer formation? As expected, substitutions (A or S) at C2 completely abrogated covalent dimer formation (Rutledge et al., 1992; Bolliger and Johansson, 1999). Furthermore, little to no noncovalent dimer was detected by two-step sequential nondenaturing IP (snIP) for these mutants (data not shown). Interestingly, a C2S mutant ζ chain associated with TCR-CD3 to form a fully assembled receptor at a level of 60% compared to WT ζ chain (Figure 5A, lanes 1 and 2). This result suggests that TCR-CD3 association can stabilize the ζζ dimer even in the absence of the native disulfide bond and explains why T cells transfected with such a ζ mutant express TCR-CD3 at the cell surface (Rutledge et al., 1992). We therefore conclude that the disulfide bond stabilizes the ζζ dimer only after formation of the proper interface and plays little to no direct role in driving dimer formation.

Are side chains involved in interface contacts also important for assembly with TCR? We analyzed reactions in which the level of ζ input mRNA was adjusted to produce similar levels of covalent dimer for all mutants

(Figure 5B, lower panel), thereby compensating for dimerization defects. With equivalent amounts of disulfide-linked ζζ dimer available, we measured the yield of fully assembled receptor complex using a two-step snIP strategy (Figure 5B, upper panel). Surprisingly, even under these conditions, several interface mutants exhibited striking defects in association with TCR-CD3 (Figure 5B, upper panel). In particular, the Y12A and T17A mutations had dramatic effects (lanes 4 and 5; 19% and 8% compared to WT), and the F20A mutant showed a lesser assembly defect (lane 6; 40% of WT). Noninterface mutations Y3A and F10A had either no effect (Y3A, 90% of WT) or only modest effects (F10A, 62% of WT) on assembly. Establishing the proper interface contacts is therefore critical not only for disulfide-linked ζζ dimer formation but also for creating the assembly-competent ζζ conformation.

The D6 Pair as a Primary TCR Contact Site

It has previously been demonstrated that the D6 pair not only is important for ζζ dimer formation but also is a primary contact for association with TCR (Rutledge et al., 1992; Call et al., 2002). Conservative substitutions (N or E) in only one strand were tolerated for ζζ dimer formation but drastically reduced assembly with TCR (Call et al., 2002). The observation that the two D6 side chains make direct contact at the $\zeta\zeta_{TM}$ dimer interface suggested that a very specific arrangement was required at this site for TCR association. We therefore evaluated the panel of one- and two-strand mutant ζζ dimers presented in Figures 3C and 3D for incorporation into a complete TCR-CD3 complex (Figure 5C). All mutant combinations exhibited dramatic assembly defects compared to WT ζζ dimer (Figure 5C). Particularly striking was the double glutamic acid substitution (EE combination), which prevented assembly with TCR even though the glutamic acid side chain is only one carbon atom longer than aspartic acid.

Receptor assembly thus displays a surprisingly stringent requirement for two aspartic acid residues properly positioned in the interface. The experimentally determined χ_1 angle of D6 places the carboxyl oxygens in the interface (Figure 6A). While the χ_2 angle of D6 cannot be directly measured, steric constraints from L9 (below) and C2 (above) result in a pair of interhelical carboxyl oxygens being in very close contact (2.4 ± 0.1 Å). These inner oxygens could also be stabilized by hydrogen bonds to the backbone amide of D6 of the opposite strand. The close proximity of the aspartate side chains, the C2 disulfide bond, and the C2 backbone carbonyl oxygens may thus create a region of high local electronegativity. Interestingly, we also identified an explicit NOE to water from the backbone amide proton of D6 in the 80 ms ^{15}N-NOESY (nuclear Overhauser effect spectroscopy) spectrum of the $\zeta\zeta_{TM}$ dimer (data not shown). This was reproduced in a second ^{15}N-NOESY spectrum with 120 ms of mixing time (Figure 6B), confirming the presence of one or more water molecules in this region. This NOE to water was unique and did not result from exposure to bulk solvent because no such signal was observed for any other residues from the two neighboring N-terminal positions through 16 positions C-terminal to D6. A mutant in which both aspartic acids were substituted by asparagine was also analyzed because this conservative substitution abrogated the ability of the ζζ dimer to assemble with TCR despite efficient formation of ζζ dimer. The distinct absence of any NOE to water in the N6 region of the ^{15}N-NOESY spectrum (data not shown) is consistent with a functional role of a water molecule (or molecules) in assembly with TCR. The D6 region may therefore contain an interchain hydrogen bonding network that involves one or more water molecules in addition to the four D6 side-chain oxygens, the two C2 backbone carbonyl oxygens, and the two D6 backbone amides. Such a complex intermolecular hydrogen bonding network centered on the D6 pair may create the specific arrangement required to bind the TM arginine residue from TCRα and could account for the stringent selectivity for two aspartic acids.

DISCUSSION

For a large number of activating receptors, it appears that the critical structural information for assembly with their dimeric signaling modules is contained within the TM domains because TM peptides were assembly competent in all receptor systems studied (Call et al., 2002; Feng et al., 2005; Garrity et al., 2005). The critical feature of this assembly mechanism is the requirement for a pair of acidic residues as the ligand for a single basic TM residue. We therefore sought to define the structure of the assembly-competent state of one of these dimeric signaling modules. We now report the high-resolution structure of the ζ chain TM dimer, a key component of both the TCR-CD3 complex and the activating NK cell receptor NKp46 (Vitale et al., 1998). Sequence alignments reveal that the residues at the $\zeta\zeta_{TM}$ dimer interface are identical in the related Fcγ dimer, with the exception of a minor change at position 20 (F versus Y; Kuster et al., 1990; Rutledge et al., 1992), and the structure is thus also relevant for the large group of activating receptors that signal through the Fcγ dimer. The structure reveals several distinctive features that are of functional significance for ζζ dimerization and assembly with TCR.

A TM Helix Dimer Interface Dominated by Polar Contacts

Due to the shallow crossing angle, the dimer interface extends through almost the entire length of the TM domains. Eight residues form interchain contacts at the $\zeta\zeta_{TM}$ dimer interface, but functional experiments demonstrate that only mutations of D6, L9, Y12, T17, and F20 (to A) have substantial effects on dimer formation. That 3 of these 5 residues are polar is striking, and their critical role is underscored by the dramatic effects of mutations at D6, Y12, or T17, each of which reduces dimer formation by 75%–85%. By comparison, the effects of mutations at the two hydrophobic positions, L9 and F20, are more modest.

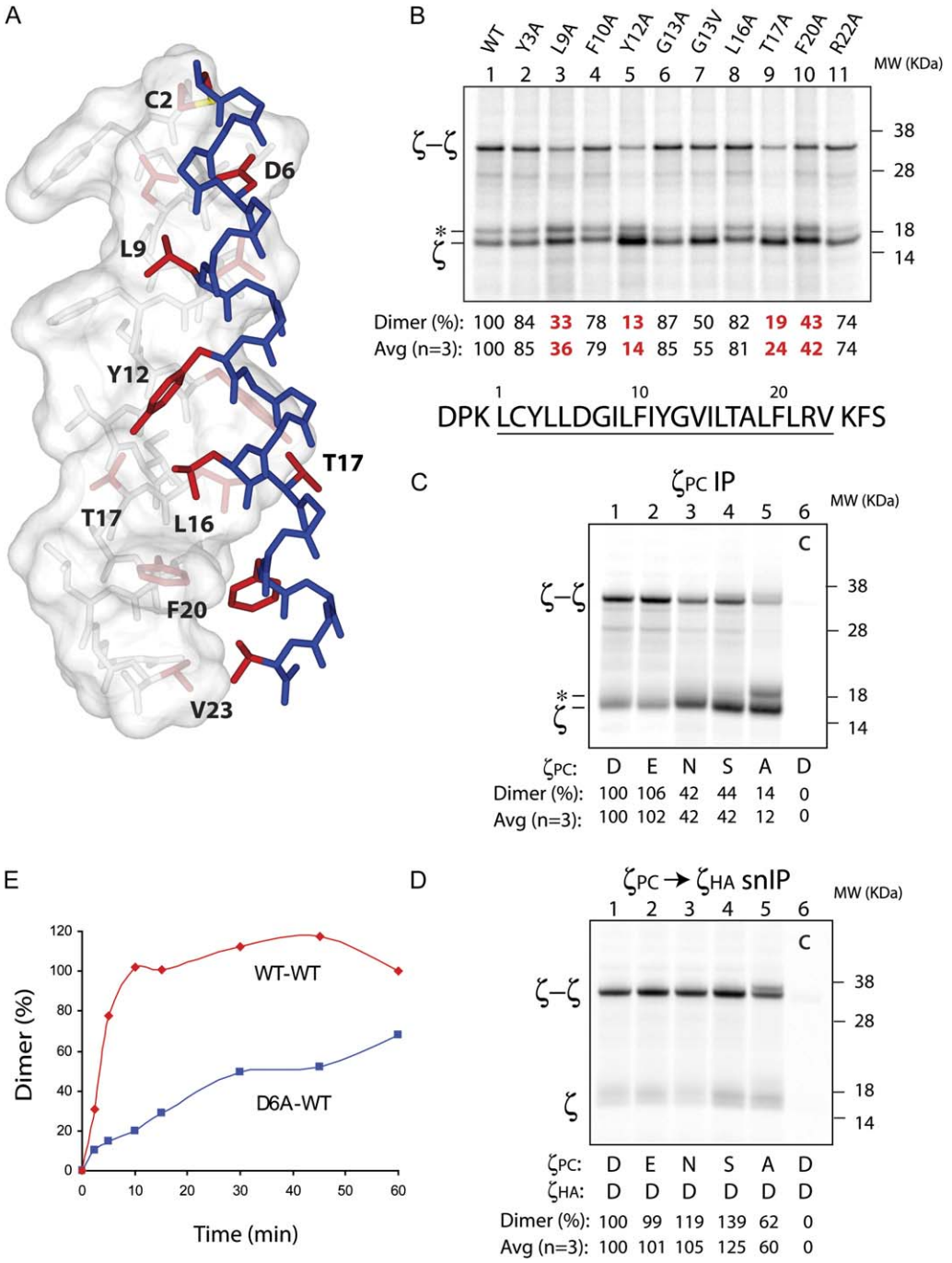

Figure 3. Definition of the $\zeta\zeta_{TM}$ Dimer Interface

(A) The entire length of the $\zeta\zeta_{TM}$ dimer interface is shown, with side chains making interface contacts labeled red. The rear strand is surface rendered to illustrate the contours of the dimer interface and contains all side chains. Side chains not involved in interface contacts have been removed from the front strand for clarity.

(B) The functional relevance of observed contacts for ζζ dimer formation was evaluated in the context of full-length wild-type (WT) ζ chain using an in vitro translation system. mRNAs encoding the indicated ζ chain WT and mutant sequences were translated in the presence of ER microsomes and allowed to assemble for 1 hr under oxidizing conditions. The membrane fraction from each reaction was analyzed by nonreducing SDS-PAGE to compare the extent of dimer formation. mRNA input was adjusted to achieve equivalent translation levels, and dimer % was calculated as a ratio of ζζ dimer to total signal in dimer plus signal-peptide-cleaved monomer bands. * indicates ζ polypeptide that is not signal-peptide cleaved and does not participate in dimer assembly. For all biochemical experiments, quantification is given for the gel shown in the figure as well as the average of three independent experiments.

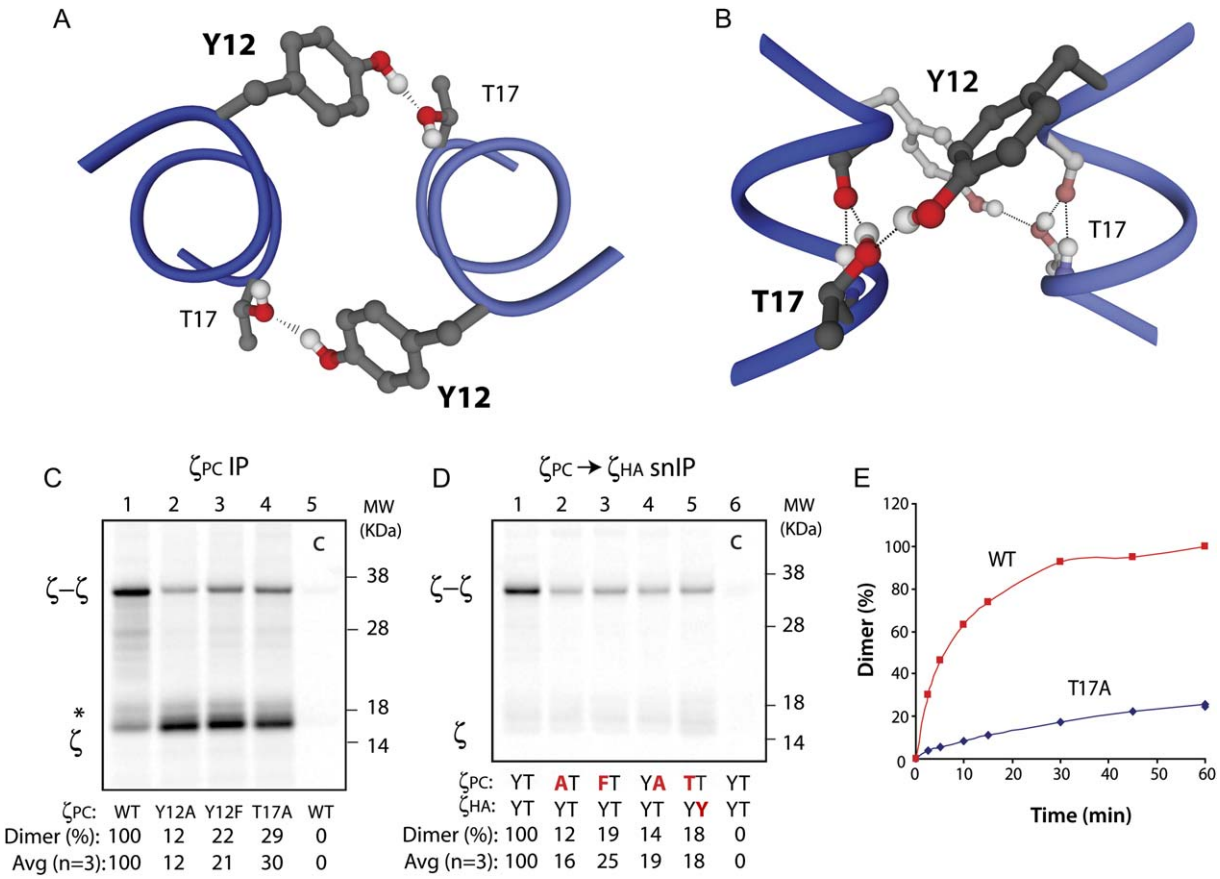

Figure 4. Two Lateral Y-T Hydrogen Bonds Are Critical for ζζ Dimerization

(A and B) The side-chain hydroxyls of Y12 and T17 form hydrogen bonds that define the lateral edges of the $\zeta\zeta_{TM}$ dimer interface. The T17 hydroxyl also forms a hydrogen bond with the backbone carbonyl oxygen of the *i*-4 residue. Views are down the dimer axis (A) or from the side (B).

(C–E) Substitution of either Y12 or T17 results in a dramatic reduction of covalent ζζ dimer formation.

(C and D) The effects of mutations in both strands (C) or only one strand (D) were evaluated by in vitro translation with ER microsomes. In (D), the positions that have been substituted are indicated in bold red type. Dimer % was calculated as in Figures 3C and 3D, respectively.

(E) The kinetics of dimer formation were analyzed as in Figure 3E for homodimers of ζ_{WT} or the T17A mutant.

The two hydroxyl-containing side chains, Y12 and T17, form interchain hydrogen bonds that create "brackets" at the edges of the dimer interface. Formation of these two Y12-T17 contacts is critical to dimer formation because removal of even a single hydroxyl group (Y12F mutation) in only one strand reduces dimer recovery by 75% compared to WT. These hydrogen bonds may be particularly strong due to the lateral proximity of the polar groups to the hydrophobic interior of the lipid bilayer. The Y12-T17 hydrogen bonds are also critical for formation of the assembly-competent ζζ dimer, as shown by assembly experiments in which dimerization defects were compensated by adjusting mRNA input. Both Y12A and T17A mutants exhibited striking defects in assembly with TCR (19% and 8% of WT, respectively), indicating that these hydrogen bonds are integral elements of the ζζ dimer structure required for interaction with TCR.

That the cysteine forming the interchain disulfide bond would make a major contribution to dimer formation appears obvious. However, our data indicate that C2 plays little (if any) role in the formation of the interface based on two criteria: (1) other mutations that disrupt the

(C–E) Contribution of a polar residue at TM position 6 to ζζ dimerization.

(C) Assembly reactions with ζ mutants in which D6 was changed to glutamic acid (E), asparagine (N), serine (S), or alanine (A) were performed as in (B). Proteins were isolated from digitonin lysates by IP with an antibody to a C-terminal protein C (PC) epitope tag and analyzed for dimer formation.

(D) The effects of these mutations were further analyzed when present in only one strand by two-step sequential nondenaturing IP (snIP) targeting the PC-tagged ζ mutant strand followed by the HA-tagged ζ_{WT} strand. Dimer % was normalized to total input ζ from a no-IP aliquot of the same reaction (data not shown). IP reactions with control antibodies (C, lane 6) were used to establish background levels.

(E) The kinetics of dimerization were compared for the ζ_{WT} and a mixed dimer in which only one strand carried the D6A mutation (D6A-WT) using the IP approach shown in (D).

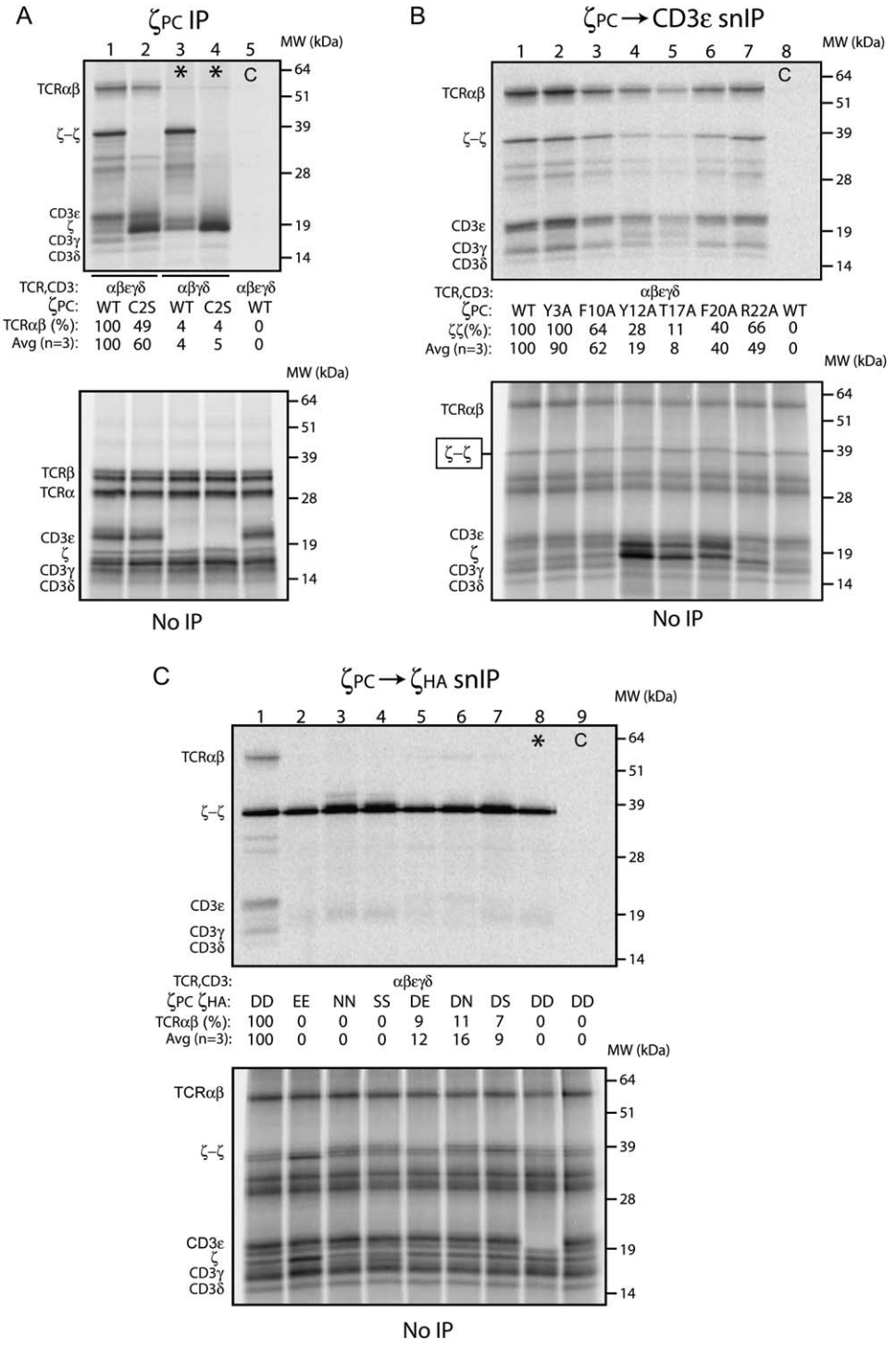

Figure 5. $\zeta\zeta_{TM}$ Structural Features that Affect Assembly with TCR-CD3

(A) The C2 disulfide bond is not required for assembly with TCR-CD3. Assembly reactions containing WT (lane 1) or C2S (lane 2) ζ_{PC} and all TCR$\alpha\beta$-CD3$\gamma\delta\varepsilon$ mRNAs were analyzed by anti-PC IP and nonreducing SDS-PAGE for assembly of complete receptor complexes. Coprecipitated TCR$\alpha\beta$ was quantitated and normalized to its expression level (lower panel), and is expressed as % of WT. Controls included translation reactions lacking CD3ε (lanes 3 and 4) and IP with a control antibody (lane 5). Lower panel shows samples of all reactions before IP separated by SDS-PAGE under reducing conditions to demonstrate input material.

(B) Mutations affecting $\zeta\zeta$ dimer formation have additional effects on assembly with TCR-CD3. Assembly reactions contained WT (lanes 1 and 8) or mutant (lanes 2–7) ζ_{PC} and all other TCR$\alpha\beta$-CD3$\gamma\delta\varepsilon$ mRNAs. Complete receptor complexes were isolated by PC (ζ)→UCHT1 (CD3ε) snIP (upper

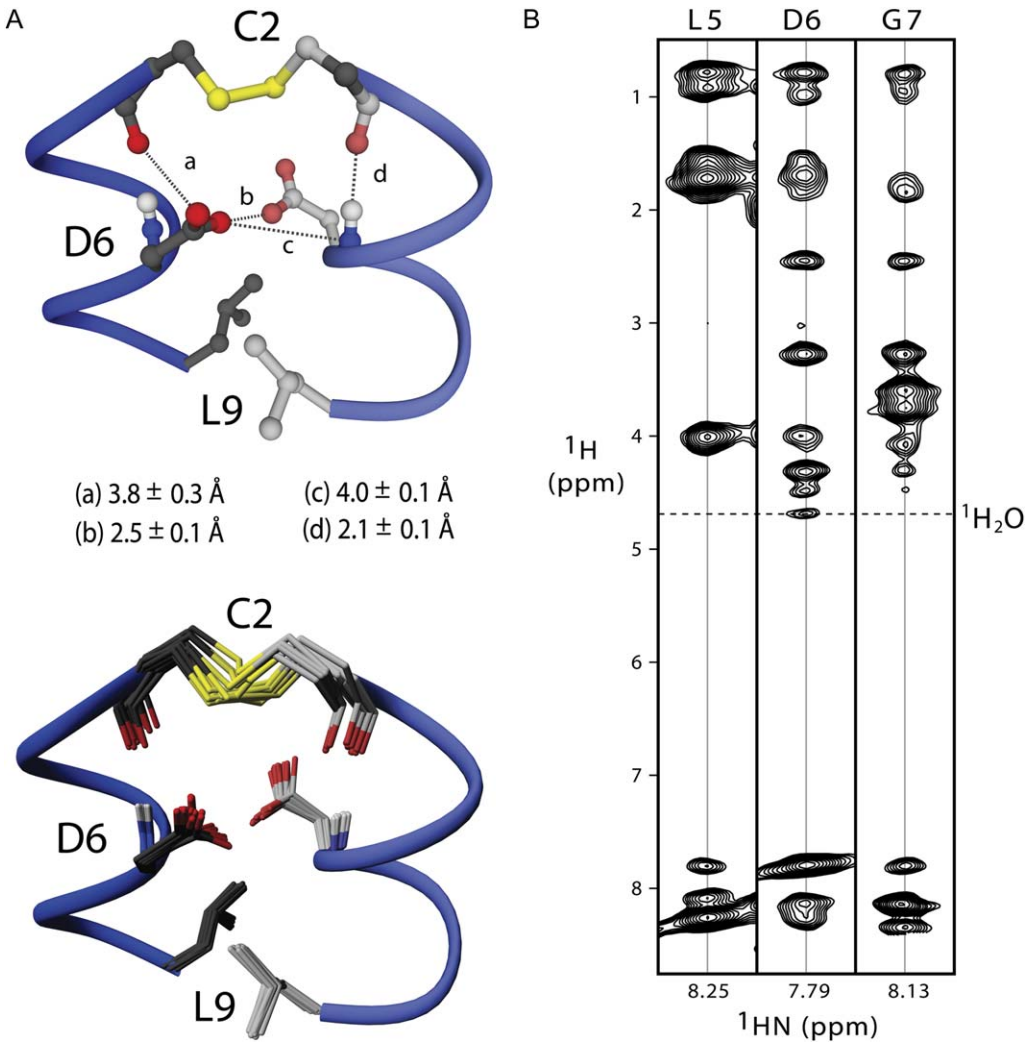

Figure 6. Structural Arrangement of the D6 Side Chains

(A) Representative structure highlighting the C2/D6 region, with other residues omitted for clarity. (Upper) Dotted lines represent the indicated distance measurements. Range of distances is given for the ensemble of 15 structures. (Lower) Ensemble view demonstrating the small experimental variation in the position of the D6 side chains in the calculated structures.

(B) Strips from a ^{15}N-NOESY spectrum (120 ms) illustrating an NOE to water from the D6 backbone amide, but not from L5 or G7.

interface prevent formation of the disulfide bond, and (2) the C2S mutant associates well with TCR (60% compared to WT) despite the absence of the interchain disulfide bond. These observations indicate that the disulfide bond stabilizes an interface shaped largely by other contacts. Interaction with TCR can thus stabilize a ζζ dimer lacking the interchain disulfide bond.

Role of the Aspartic Acid Pair in ζζ Dimerization

Mutation of D6 to alanine in both strands (AA) causes a profound defect in dimer formation (12% of WT), consistent with previous studies in cellular systems (Rutledge et al., 1992). Surprisingly, even a conservative substitution from aspartic acid to asparagine (NN) reduces dimerization to ~40% of WT, and the aspartic acid + alanine combination

panel). ζζ dimer recovered in the full complex was quantitated and normalized to its input level (lower panel). Lane 8 presents an IP with an isotype control antibody. Lower panel shows samples of all reactions before IP separated under nonreducing conditions to demonstrate equal levels of ζζ dimer (boxed).

(C) Assembly reactions contained TCRαβ and CD3εγδ as well as PC- or HA-tagged ζ chain mRNAs encoding either the WT TM sequence or a substitution of D6 by E, N, or S. The indicated ζζ dimer was isolated by PC→HA snIP, and associated TCRαβ was quantitated and normalized to its expression level. Lane 8 is a control in which ζζ and TCR-CD3 were translated in separate reactions and mixed before IP analysis. Lane 9 is the isotype control antibody IP.

(DA) yields higher levels of ζζ dimer (60%) than either the double asparagine (NN, 42%) or double serine (SS, 42%) mutants. The DA combination may be more favorable than AA due to an interchain hydrogen bond between the D6 side chain and the position 6 backbone amide of the opposite strand. Efficient dimer formation thus requires a combination of at least one acidic residue and a polar residue at position 6 in the two strands. Although close packing of two acidic groups at the interface is initially surprising, studies with model TM peptides demonstrated that similar interactions can drive oligomerization within the membrane (Gratkowski et al., 2001; Zhou et al., 2001). However, asparagine and glutamine were superior to aspartic and glutamic acid in these studies and, in the best case (asparagine), trimers prevailed over dimers. Thus, the similarity to the $\zeta\zeta_{TM}$ dimer may be rather limited. It is apparent that access to the D6 site for a receptor-donated arginine may be occluded by the Y3 and L5 side chains. This feature may help to stabilize the ζζ dimer before assembly with the receptor, and adoption of alternative side-chain conformations at these positions upon receptor binding may provide better access to the critical site.

The Aspartic Acid Pair as the Primary TCR Binding Site

Assembly of ζζ with TCR is exquisitely selective for a particular structure that is only formed by two aspartic acids at position 6 and is thus considerably more stringent than the requirements for ζζ dimer formation. Perhaps most strikingly, WT levels of ζζ dimer are formed by the position 6 glutamic acid mutant (EE combination), but this dimer shows no interaction with TCR. These observations pose two related questions: Which structural features account for the selectivity for an aspartic acid pair in assembly with TCR, and how is the close packing of two acidic groups stabilized? In the $\zeta\zeta_{TM}$ structure, the aspartic acid side chains make favorable hydrogen bonds to the backbone amide groups of the opposite strand, which could provide significant stabilization. Close apposition of acidic groups in soluble proteins is often stabilized by shared protons, bound water molecules, or coordinated counter-ions. It has been suggested that the acidic pairs in the CD3 and $\zeta\zeta_{TM}$ domains are in a state of partial ionization, sharing a proton and therefore bearing a net charge of −1 (Senes et al., 2004). While this is entirely possible in our structure, we have no direct spectroscopic evidence to support a shared proton. The presence of a unique water signal within close proximity to D6 strongly suggests that a water molecule (or molecules) plays a structural role in stabilizing the aspartic acid pair and may also serve as a component of the structural unit recognized by the TCRα arginine. At present, we cannot determine how many water molecules are present in the vicinity of the D6 pair, and we have therefore refrained from building explicit molecular models.

If one or more water molecules participate in an interchain hydrogen bonding network orchestrated by the D6 side chains, such a structural arrangement could account for the selectivity of receptor assembly. Water molecules bound by aspartic acid pairs are known to play critical roles in both soluble and membrane protein structures. In the high-resolution crystal structure of bacteriorhodopsin (Luecke et al., 1999), the membrane-embedded light-driven proton pump from *Halobacterium salinarium*, a network of hydrogen bonds is formed by two critical aspartic acids (D85 and D212), the protonated Schiff base, and several water molecules, and this arrangement is critical for proton transport across the membrane. Classical aspartyl proteases such as HIV-1 protease use two active-site aspartic acids to coordinate and activate a water molecule for nucleophilic attack on the peptide bond (Pillai et al., 2001). The presenilins are intramembrane aspartyl proteases that form the proteolytic subunit of γ-secretase and are thought to perform intramembrane peptide-bond hydrolysis through two catalytic aspartic acids buried in the center of neighboring TM domains (Wolfe et al., 1999). These aspartic acids must therefore coordinate a water molecule in a similar manner within the membrane environment. The structure of the $\zeta\zeta_{TM}$ dimer demonstrates that the two aspartic acids required for receptor assembly form a single structural unit involving other hydrogen-bond donors and acceptors. A high-resolution structure of an assembled complex will be required to determine how the basic side chain interacts with this structural unit and whether one or more structural water molecules and/or protons participate in this assembly.

EXPERIMENTAL PROCEDURES

Protein Production and Reconstitution

The 33 amino acid ζ_{TM} peptide (DSKLCYLLDGILFIYGVILTALFLRV KFSRSAD) was expressed as a C-terminal in-frame fusion to the trpLE sequence with an N-terminal 9-His tag in the pMM-LR6 vector (gift from S.C. Blacklow, Harvard Medical School, Boston). Transformed *E. coli* BL21(DE3) cells were inoculated into 500 ml M9 minimal medium with Centrum multivitamins and one or more stable isotope labels in 2.0 l baffled flasks. Cultures were grown at 37°C to OD_{600} ~ 0.6 and cooled to 20°C for 1 hr before overnight induction at 20°C with 125 μM IPTG. Full deuteration of the ζ_{TM} peptide required growth in D_2O with deuterated glucose (Cambridge Isotope Laboratories, Andover, MA, USA). Inclusion bodies were extracted with 6 M guanidine HCl, 50 mM Tris (pH 8.0), 200 mM NaCl, 1% Triton X-100, and 5 mM 2-mercaptoethanol. The cleared lysate was bound to a Ni^{2+} affinity column (Sigma) and washed with 8 M urea. The column was then incubated for 1 hr at room temperature in a urea solution containing 20 μM $CuSO_4$ and 2 mM oxidized glutathione, which was then washed out with water before elution in 70% formic acid. Digest with CNBr in 70% formic acid (2 hr, 0.2 g/ml) liberated the ζ_{TM} peptide from the trpLE fusion partner. The digest was dialyzed to water, lyophilized, and loaded onto a C4 column (Grace-Vydac) in 50% trifluoroacetic acid (TFA). Fragments were separated on a gradient of 40%–95% acetonitrile (0.1% TFA), and the $\zeta\zeta_{TM}$ peptide dimer was identified by mass spectrometry. NMR samples were prepared with 1–2 mg of lyophilized $\zeta\zeta_{TM}$ peptide dimer in 20–40 mM D25-SDS followed by addition of 5× D38-DPC (deuterated detergents from Cambridge Isotope Laboratories). All solutions contained 20 mM sodium phosphate at pH 7.0 and 5% D_2O. Final concentration of surfactant was 120–240 mM. Samples were placed in 280 μl Shigemi microcells.

NMR Measurements and Structure Calculation

All NMR spectra were collected at 30°C on Bruker spectrometers operating at ^{1}H frequencies of 500 MHz or 600 MHz and equipped with cryogenic probes. Distance restraints were obtained from ^{15}N-NOESY spectra with mixing times of 80 and 120 ms and a ^{13}C-NOESY spectrum with a mixing time of 150 ms. Interhelical distance restraints were obtained from a ^{15}N-NOESY spectrum with a mixing time of 200 ms, recorded using the 1:1 (^{2}H, ^{15}N):^{1}H mixed-label dimer. Side-chain χ_1 and χ_2 rotamers were obtained from measurements of the three-bond scalar couplings (Bax et al., 1994). For determining χ_1 rotamers for residues other than Thr, Val, and Ile, quantative J approaches based on the ^{1}H-^{15}N HSQC were used to measure $^{3}J_{C'C_\gamma}$ and $^{3}J_{NC_\gamma}$ coupling constants (Hu et al., 1997a, 1997b). For $^{3}J_{C'C_\gamma}$ and $^{3}J_{NC_\gamma}$ of Thr, Val, and Ile and $^{3}J_{C_\alpha C_\delta}$ (used to derive the χ_2 rotamers) of Leu and Ile, 2D spin-echo difference methods based on ^{1}H-^{13}C constant-time HSQC were employed (Grzesiek et al., 1993; Vuister et al., 1993; MacKenzie et al., 1996). The $^{3}J_{C'C'_\gamma}$ of D6 was measured using a 3D HN(CO)CO experiment (Hu and Bax, 1996). For RDC measurements, weak alignment of the micelle-reconstituted $\zeta\zeta_{TM}$ was accomplished using a modified version (Chou et al., 2001) of the strain-induced alignment in a gel (SAG) method (Tycko et al., 2000). Two types of backbone RDCs, $^{1}D_{NH}$ and $^{1}D_{C_\alpha H_\alpha}$, were measured.

Refinement was performed with the program XPLOR-NIH (Schwieters et al., 2003). A high-temperature (from 1000 to 200 K) annealing of the dimer was run to satisfy NOE and dihedral restraints. The quality of the structures at this step was independently validated by a singular-value decomposition fit of all RDCs to the 15 (out of 30) lowest energy dimers, resulting in a Pearson correlation coefficient of 0.96 and a free quality factor of 0.24 (Cornilescu et al., 1998). To further improve the agreement with the experimental data, each of these 15 structures was put through a low-temperature (from 200 to 20 K) refinement in which the force constants for RDCs were ramped up and all other types of restraints were kept fixed. The lowest energy structures (out of 10) were chosen for the final ensemble. The structures were superimposed over all heavy backbone atoms in residues 1–25, and the structure closest to the mean was chosen as representative. Refinement statistics of the 15 final structures are given in Table 1. A detailed description of data collection and structure calculation can be found in the Supplemental Experimental Procedures.

In Vitro Transcription, Translation, and Assembly

Full-length human ζ chain and mutant sequences were cloned into a modified pSP64 vector for in vitro translation with C-terminal peptide affinity tags as previously described (Call et al., 2002). In vitro transcription, translation, and IP/snIP analyses were performed as described in Call et al. (2002) and in the Supplemental Experimental Procedures.

Supplemental Data

Supplemental Data include Supplemental Experimental Procedures, Supplemental References, one figure, and one table and can be found with this article online at http://www.cell.com/cgi/content/full/127/2/355/DC1/.

ACKNOWLEDGMENTS

The NMR data were collected using spectrometers at the Center for Magnetic Resonance at the Massachusetts Institute of Technology (National Institutes of Health grant EB002026). M.E.C. would like to thank Dr. Melissa J. Nicholson for helpful discussion and valuable technical advice. This work was supported by a grant from the National Institutes of Health (RO1 AI054520) to K.W.W. J.R.S. acknowledges an F32 NIH fellowship. J.J.C. is the recipient of a Pew Scholarship and the Alexander and Margaret Stewart Trust Award.

Received: June 13, 2006
Revised: July 23, 2006
Accepted: August 11, 2006
Published: October 19, 2006

REFERENCES

Alcover, A., Mariuzza, R.A., Ermonval, M., and Acuto, O. (1990). Lysine 271 in the transmembrane domain of the T-cell antigen receptor beta chain is necessary for its assembly with the CD3 complex but not for alpha/beta dimerization. J. Biol. Chem. *265*, 4131–4135.

Bax, A., Vuister, G.W., Grzesiek, S., Delaglio, F., Wang, A.C., Tschudin, R., and Zhu, G. (1994). Measurement of homo- and heteronuclear J couplings from quantitative J correlation. Methods Enzymol. *239*, 79–105.

Blumberg, R.S., Alarcon, B., Sancho, J., McDermott, F.V., Lopez, P., Breitmeyer, J., and Terhorst, C. (1990). Assembly and function of the T cell antigen receptor. Requirement of either the lysine or arginine residues in the transmembrane region of the alpha chain. J. Biol. Chem. *265*, 14036–14043.

Bolliger, L., and Johansson, B. (1999). Identification and functional characterization of the zeta-chain dimerization motif for TCR surface expression. J. Immunol. *163*, 3867–3876.

Call, M.E., Pyrdol, J., Wiedmann, M., and Wucherpfennig, K.W. (2002). The organizing principle in the formation of the T cell receptor-CD3 complex. Cell *111*, 967–979.

Call, M.E., Pyrdol, J., and Wucherpfennig, K.W. (2004). Stoichiometry of the T-cell receptor-CD3 complex and key intermediates assembled in the endoplasmic reticulum. EMBO J. *23*, 2348–2357.

Chou, J.J., Gaemers, S., Howder, B., Louis, J.M., and Bax, A. (2001). A simple apparatus for generating stretched polyacrylamide gels, yielding uniform alignment of proteins and detergent micelles. J. Biomol. NMR *21*, 377–382.

Cornilescu, G., Marquardt, J.L., Ottiger, M., and Bax, A. (1998). Validation of protein structure from anisotropic carbonyl chemical shifts in a dilute liquid crystalline phase. J. Am. Chem. Soc. *120*, 6836–6837.

Cosson, P., Lankford, S.P., Bonifacino, J.S., and Klausner, R.D. (1991). Membrane protein association by potential intramembrane charge pairs. Nature *351*, 414–416.

Dietrich, J., Neisig, A., Hou, X., Wegener, A.M., Gajhede, M., and Geisler, C. (1996). Role of CD3 gamma in T cell receptor assembly. J. Cell Biol. *132*, 299–310.

Exley, M., Terhorst, C., and Wileman, T. (1991). Structure, assembly and intracellular transport of the T cell receptor for antigen. Semin. Immunol. *3*, 283–297.

Feng, J., Garrity, D., Call, M.E., Moffett, H., and Wucherpfennig, K.W. (2005). Convergence on a distinctive assembly mechanism by unrelated families of activating immune receptors. Immunity *22*, 427–438.

Garrity, D., Call, M.E., Feng, J., and Wucherpfennig, K.W. (2005). The activating NKG2D receptor assembles in the membrane with two signaling dimers into a hexameric structure. Proc. Natl. Acad. Sci. USA *102*, 7641–7646.

Geisler, C., Kuhlmann, J., and Rubin, B. (1989). Assembly, intracellular processing, and expression at the cell surface of the human alpha beta T cell receptor/CD3 complex. Function of the CD3-zeta chain. J. Immunol. *143*, 4069–4077.

Gratkowski, H., Lear, J.D., and DeGrado, W.F. (2001). Polar side chains drive the association of model transmembrane peptides. Proc. Natl. Acad. Sci. USA *98*, 880–885.

Grzesiek, S., Vuister, G.W., and Bax, A. (1993). A simple and sensitive experiment for measurement of JCC couplings between backbone carbonyl and methyl carbons in isotopically enriched proteins. J. Biomol. NMR *3*, 487–493.

Hu, J.-S., and Bax, A. (1996). Measurement of three-bond 13C-13C J couplings between carbonyl and carbonyl/carboxyl carbons in isotopically enriched proteins. J. Am. Chem. Soc. *118*, 8170–8171.

Hu, J.-S., Grzesiek, S., and Bax, A. (1997a). chi1 angle information from a simple two-dimensional NMR experiment which identifies trans 3JNCg couplings in isotopically enriched proteins. J. Biomol. NMR *9*, 323–328.

Hu, J.-S., Grzesiek, S., and Bax, A. (1997b). Two-dimensional NMR methods for determining c1 angles of aromatic residues in proteins from three-bond JC′Cg and JNCg couplings. J. Am. Chem. Soc. *119*, 1803–1804.

Ishikawa, S., Arase, N., Suenaga, T., Saita, Y., Noda, M., Kuriyama, T., Arase, H., and Saito, T. (2004). Involvement of FcRgamma in signal transduction of osteoclast-associated receptor (OSCAR). Int. Immunol. *16*, 1019–1025.

Kearse, K.P., Roberts, J.L., and Singer, A. (1995). TCR alpha-CD3 delta epsilon association is the initial step in alpha beta dimer formation in murine T cells and is limiting in immature CD4+ CD8+ thymocytes. Immunity *2*, 391–399.

Kuster, H., Thompson, H., and Kinet, J.P. (1990). Characterization and expression of the gene for the human Fc receptor gamma subunit. Definition of a new gene family. J. Biol. Chem. *265*, 6448–6452.

Lanier, L.L. (2005). NK cell recognition. Annu. Rev. Immunol. *23*, 225–274.

Lanier, L.L., Corliss, B.C., Wu, J., Leong, C., and Phillips, J.H. (1998a). Immunoreceptor DAP12 bearing a tyrosine-based activation motif is involved in activating NK cells. Nature *391*, 703–707.

Laskowski, R.A., MacArthur, M.W., Moss, D.S., and Thornton, J.M. (1993). PROCHECK: a program to check the stereochemical quality of protein structures. J. Appl. Crystallogr. *26*, 283–291.

Lemmon, M.A., Flanagan, J.M., Hunt, J.F., Adair, B.D., Bormann, B.J., Dempsey, C.E., and Engelman, D.M. (1992a). Glycophorin A dimerization is driven by specific interactions between transmembrane alpha-helices. J. Biol. Chem. *267*, 7683–7689.

Lemmon, M.A., Flanagan, J.M., Treutlein, H.R., Zhang, J., and Engelman, D.M. (1992b). Sequence specificity in the dimerization of transmembrane alpha-helices. Biochemistry *31*, 12719–12725.

Luecke, H., Schobert, B., Richter, H.T., Cartailler, J.P., and Lanyi, J.K. (1999). Structure of bacteriorhodopsin at 1.55 A resolution. J. Mol. Biol. *291*, 899–911.

MacKenzie, K.R., Prestegard, J.H., and Engelman, D.M. (1996). Leucine side-chain rotamers in a glycophorin A transmembrane peptide as revealed by three-bond carbon-carbon couplings and 13C chemical shifts. J. Biomol. NMR *7*, 256–260.

MacKenzie, K.R., Prestegard, J.H., and Engelman, D.M. (1997). A transmembrane helix dimer: structure and implications. Science *276*, 131–133.

Oxenoid, K., and Chou, J.J. (2005). The structure of phospholamban pentamer reveals a channel-like architecture in membranes. Proc. Natl. Acad. Sci. USA *102*, 10870–10875.

Pillai, B., Kannan, K.K., and Hosur, M.V. (2001). 1.9 A x-ray study shows closed flap conformation in crystals of tethered HIV-1 PR. Proteins *43*, 57–64.

Popot, J.L., Gerchman, S.E., and Engelman, D.M. (1987). Refolding of bacteriorhodopsin in lipid bilayers. A thermodynamically controlled two-stage process. J. Mol. Biol. *198*, 655–676.

Punt, J.A., Roberts, J.L., Kearse, K.P., and Singer, A. (1994). Stoichiometry of the T cell antigen receptor (TCR) complex: each TCR/CD3 complex contains one TCR alpha, one TCR beta, and two CD3 epsilon chains. J. Exp. Med. *180*, 587–593.

Rutledge, T., Cosson, P., Manolios, N., Bonifacino, J.S., and Klausner, R.D. (1992). Transmembrane helical interactions: zeta chain dimerization and functional association with the T cell antigen receptor. EMBO J. *11*, 3245–3254.

Samelson, L.E., Harford, J.B., and Klausner, R.D. (1985). Identification of the components of the murine T cell antigen receptor complex. Cell *43*, 223–231.

Schwieters, C.D., Kuszewski, J.J., Tjandra, N., and Marius Clore, G. (2003). The Xplor-NIH NMR molecular structure determination package. J. Magn. Reson. *160*, 65–73.

Senes, A., Engel, D.E., and DeGrado, W.F. (2004). Folding of helical membrane proteins: the role of polar, GxxxG-like and proline motifs. Curr. Opin. Struct. Biol. *14*, 465–479.

Staley, J.P., and Kim, P.S. (1994). Formation of a native-like subdomain in a partially folded intermediate of bovine pancreatic trypsin inhibitor. Protein Sci. *3*, 1822–1832.

Sussman, J.J., Bonifacino, J.S., Lippincott-Schwartz, J., Weissman, A.M., Saito, T., Klausner, R.D., and Ashwell, J.D. (1988). Failure to synthesize the T cell CD3-zeta chain: structure and function of a partial T cell receptor complex. Cell *52*, 85–95.

Tomasello, E., Olcese, L., Vely, F., Geourgeon, C., Blery, M., Moqrich, A., Gautheret, D., Djabali, M., Mattei, M.G., and Vivier, E. (1998). Gene structure, expression pattern, and biological activity of mouse killer cell activating receptor-associated protein (KARAP)/DAP-12. J. Biol. Chem. *273*, 34115–34119.

Tycko, R., Blanco, F.J., and Ishii, Y. (2000). Alignment of biopolymers in strained gels: A new way to create detectable dipole-dipole couplings in high-resolution biomolecular NMR. J. Am. Chem. Soc. *122*, 9340–9341.

Vitale, M., Bottino, C., Sivori, S., Sanseverino, L., Castriconi, R., Marcenaro, E., Augugliaro, R., Moretta, L., and Moretta, A. (1998). NKp44, a novel triggering surface molecule specifically expressed by activated natural killer cells, is involved in non-major histocompatibility complex-restricted tumor cell lysis. J. Exp. Med. *187*, 2065–2072.

Vuister, G.W., Wang, A.C., and Bax, A. (1993). Measurement of three-bond nitrogen-carbon J couplings in proteins uniformly enriched in nitrogen-15 and carbon-13. J. Am. Chem. Soc. *115*, 5334–5335.

Walters, K.J., Matsuo, H., and Wagner, G. (1997). A simple method to distinguish intermonomer nuclear overhauser effects in homodimeric proteins with c2 symmetry. J. Am. Chem. Soc. *119*, 5958–5959.

Weissman, A.M., Baniyash, M., Hou, D., Samelson, L.E., Burgess, W.H., and Klausner, R.D. (1988). Molecular cloning of the zeta chain of the T cell antigen receptor. Science *239*, 1018–1021.

Wolfe, M.S., Xia, W., Ostaszewski, B.L., Diehl, T.S., Kimberly, W.T., and Selkoe, D.J. (1999). Two transmembrane aspartates in presenilin-1 required for presenilin endoproteolysis and gamma-secretase activity. Nature *398*, 513–517.

Wu, J., Song, Y., Bakker, A.B., Bauer, S., Spies, T., Lanier, L.L., and Phillips, J.H. (1999). An activating immunoreceptor complex formed by NKG2D and DAP10. Science *285*, 730–732.

Zhou, F.X., Merianos, H.J., Brunger, A.T., and Engelman, D.M. (2001). Polar residues drive association of polyleucine transmembrane helices. Proc. Natl. Acad. Sci. USA *98*, 2250–2255.

Accession Numbers

The structures described herein have been deposited in the Protein Data Bank with ID code 2HAC.

Cell, Volume *127*

Supplemental Data

The Structure of the ζζ Transmembrane Dimer Reveals Features Essential for Its Assembly with the T Cell Receptor

Matthew E. Call, Jason R. Schnell, Chenqi Xu, Regina A. Lutz, James J. Chou, and Kai W. Wucherpfennig

Supplemental Experimental Procedures

NMR Measurements

All NMR data were collected at 30 °C on Bruker spectrometers operating at ^{1}H frequencies of 500 MHz or 600 MHz and equipped with cryogenic probes. Data processing and spectra analyses were done in NMRPipe (Delaglio et al., 1995) and XEASY (Bartels et al., 1995). Fitting of the dipolar couplings to structures was done by singular value decomposition (Losonczi et al., 1999), using the program PALES (Zweckstetter and Bax, 2000). The goodness of fit was assessed by both Pearson correlation coefficient (*r*) and the quality factor (Q) (Cornilescu et al., 1998).

Sequence-specific backbone amide resonance assignments were determined from the gradient-selected TROSY-HNCA (Kay et al., 1990; Salzmann et al., 1999) collected on a uniform ^{15}N-,^{13}C-, and 85% ^{2}H-labeled sample. Backbone amide resonance assignments were confirmed and extended to side chain protons in an ^{15}N-edited NOESY spectrum with 80 ms of mixing time, recorded using a uniform ^{15}N-, ^{13}C-labeled sample. Stereospecific assignment of methyl groups were obtained by collecting a constant-time (28 ms) ^{1}H,^{13}C-HSQC on 10% ^{13}C-labeled protein (Szyperski et al., 1992). Intramolecular distance restraints were obtained from the ^{15}N-edited NOESY spectrum and a ^{13}C-edited NOESY spectrum with 150 ms of mixing time, recorded using a uniform ^{15}N-, ^{13}C-labeled sample. Intermolecular NOEs between backbone amide protons of ^{15}N-, ^{2}H-labeled monomer and non-exchangeable side chain protons of unlabeled monomer were obtained from an ^{15}N-edited NOESY spectrum with 200 ms of mixing time on a mixed-label (uniformly ^{15}N/^{2}H and unlabeled) dimer (Walters et al., 1997). An additional ^{15}N-edited NOESY spectrum with 120 ms of mixing time was collected to confirm the presence of the water NOE to the backbone amide of D6 that was detected in the 80 ms mixing time NOESY.

Side chain χ_1 rotamers were extracted from $^{3}J_{C'C\gamma}$ and $^{3}J_{NC\gamma}$ coupling constants. Side chain χ_2 rotamers of Leu and Ile residues were extracted from $^{3}J_{C\alpha C\delta}$coupling contants. For measurements of $^{3}J_{NC\gamma}$ coupling constants for determining side chain χ_1 rotamers for residues other than Thr, Val, and Ile, quantitative-*J* approaches based on 2D ^{1}H-^{15}N constant-time TROSY were used

(Hu et al., 1997a; Hu et al., 1997b). For $^3J_{C'C\gamma}$ and $^3J_{NC\gamma}$ of Thr, Val, and Ile, and $^3J_{C\alpha C\delta}$ of Leu and Ile, 2D spin-echo difference methods based on ^{1}H-^{13}C constant-time HSQC were employed (Grzesiek et al., 1993; MacKenzie et al., 1996; Vuister et al., 1993). In addition, the χ_1 of D6 was determined by measuring the carbonyl-to-carboxyl ^3J coupling constant using a modified TROSY version of the 3D HN(CO)CO experiment (Hu and Bax, 1996). All 3-bond couplings are given in Supplementary Table 1.

For RDC measurements, weak alignment of the protein-micelle complex was accomplished using a modified version (Chou et al., 2001) of the strain-induced alignment in a gel (SAG) method (Sass et al., 2000; Tckyo et al., 2000). The protein/surfactant solution was soaked into a cylindrically shaped polyacrylamide gel (5% acrylamide concentration and acrylamide/bisacrylamide molar ratio of 80), initially of 6 mm diameter and 9 mm length, which was subsequently radially compressed to fit within the 4.2 mm inner diameter of a NMR tube with open ends (http://newera-spectro.com), thereby increasing its length to 18 mm. The ^{1}H-^{15}N J+D couplings were measured at 600 MHz (^{1}H frequency) by interleaving a regular gradient-enhanced HSQC and a gradient-selected TROSY, both acquired with 80 ms of ^{15}N evolution. The $^1H_\alpha$-$^{13}C_\alpha$ J+D couplings were measured at 500 MHz (^{1}H frequency) using a 2D (CA)CONH quantitative J_{CH} experiment with interleaved spectra recorded at J_{CH} modulation of 1.83, 3.63, and 7.12 ms. This experiment was modified from the 3D CB(CA)CONH quantitative J_{CH} experiment (Chou and Bax, 2001) used primarily for measuring $^1H_\beta$-$^{13}C_\beta$ J+D couplings. The (CA)CONH was optimized for measuring $^1H_\alpha$-$^{13}C_\alpha$ couplings only.

NMR Structure Calculation

Structure calculation was performed using the program XPLOR-NIH (Schwieters et al., 2003). The complete protocol consists of a high-temperature annealing to satisfy NOE and dihedral restraints and a low-temperature refinement to satisfy RDCs and all other restraints. In the high-temperature run, the bath is cooled from 1000 to 300 K with a temperature step of 20 K. Experimental data consisted of distance restraints from NOEs, and side-chain χ_1 and χ_2 angles from $^3J_{NC\gamma}$, $^3J_{C'C\gamma}$, and $^3J_{C\alpha C\delta}$scalar couplings. Intra-molecular distances derived from the ^{15}N-edited and ^{13}C-edited NOESY spectra were enforced by ±0.55 or ±1.0 Å flat-well harmonic potentials. Inter-molecular distances derived from the mixed-label sample were enforced by ±0.75 Å flat-well harmonic potentials. All distance restraint force constants were ramped from 5 to 100 kcal mol^{-1} Å^{-2}. Side chain rotamers were enforced as flat-well (±20-30˚) harmonic potentials with the force constant ramped from 5 to 40 kcal mol^{-1} rad^{-2}. In addition, a weak database-derived 'rama' potential function (Kuszewski et al., 1997) was ramped from 0.02 to 0.2 (dimensionless force constant) for the general treatment of side chain rotamers. Other force constants included: k(van der Waals) = 0.002 → 4.0 kcal mol^{-1} Å^{-2}, k(improper) = 0.1 → 1.0 kcal mol^{-1} degree^{-2}, and k(bond angle) = 0.4 → 1.0 kcal mol^{-1} degree^{-2}. An ensemble of 30 structures was calculated.

The lowest energy NOE- and dihedral-derived structure from above was used as the starting model for RDC refinement at low temperature using a previously established protocol (Chou et al., 2000). In this stage, the bath was cooled from 300 to 20 K, the NOE restraint force constant was ramped down from 100 to 30 kcal mol^{-1} Å^{-2}. The side chain dihedral force constant was kept the same at 40 kcal mol^{-1} rad^{-2}. RDC restraint force constant was ramped from 0.0002 to 0.0160 kcal mol^{-1} Hz^{-2} (normalized for the $^1D_{NH}$ couplings). All other force constants are the same as the

values at the end of the high-temperature annealing run. An ensemble of 30 structures was refined. The final ensemble consisted of the 15 lowest energy structures. The structures were superimposed over all heavy backbone atoms in residues 1-25 and the structure closest to the mean was chosen as representative. Refinement statistics of the 15 final structures are given in Table 1.

In Vitro Transcription, Translation, and Assembly

Full-length human ζ chain and mutant sequences were cloned into a modified pSP64 vector for *in vitro* translation with C-terminal peptide affinity tags as previously described (Call et al, 2002). *In vitro* transcription was performed from linearized cDNA constructs using RiboMax T7 Large-Scale RNA Production kit and methyl-^{7}G cap analog (Promega; Madison, WI). Each 25 μl translation reaction contained 17.5 μl nuclease-treated rabbit reticulocyte lysate (Promega), 0.5 μl amino acid mixture minus methionine/cysteine (Promega), 0.5 μl SUPERase-In RNase inhibitor (Ambion, Austin, TX), 1-2 μl [^{35}S]-labeled methionine/cysteine (Pro-Mix, Amersham; Piscataway, NJ), mRNA and 2.0 μl ER microsomes from a murine hybridoma (IVD12) which were isolated as previously described (Call et al, 2002). Some experiments were performed using canine pancreas rough microsomes (provided by M. Wiedmann, Memorial Sloan-Kettering Cancer Center, New York, NY) for improved signal peptide cleavage with D6 mutants. All *in vitro* translation and assembly reactions were performed at 30°C. An initial translation period of 30 minutes under reducing conditions was followed by a 1-4 hour assembly period after addition of oxidized glutathione to 4 mM. Reaction volumes were 25 to 75 μl as required for optimal signal with multi-step snIP procedures.

Immunoprecipitation, Electrophoretic Analysis, and Densitometry

The following mAbs directed against epitope tags were used for IP procedures: High-affinity anti-HA (rat mAb 3F10) and calcium-dependent anti-PC (mouse mAb HPC4) from Roche (Indianapolis, IN), as well as anti-CD3ε (mouse mAb UCH-T1) from Santa Cruz (Santa Cruz, CA). Translation and assembly reactions were stopped with 1 ml ice-cold Tris-buffered saline (TBS)/10 mM iodoacetamide, and microsomes were pelleted (10 min/20,000 g/4°C) and rinsed. Pellets were solubilized in 400 μl IP buffer (TBS + 0.5% digitonin [Biosynth International, Naperville, IL], 10 mM iodoacetamide, 0.1% BSA, 5 μg/ml leupeptin, 1 mM PMSF; with 1 mM $CaCl_2$ when anti-PC mAb was used) for 30 min rotating at 4°C. Lysates were pre-cleared for 1 hour with Tris/BSA-blocked Sepharose 4 beads, and primary captures were performed overnight at 4°C. Primary IP products were washed twice in 0.5 ml wash buffer (TBS + 0.5% digitonin, 10 mM iodoacetamide; with 1 mM $CaCl_2$ for anti-Protein C mAb binding). Non-denaturing elution with EDTA (PC tag) was performed as described (Call et al, 2002), and eluted complexes were incubated with subsequent antibodies and Protein G-Sepharose 4 beads (Amersham) for 2 hours at 4°C and washed. Final precipitates from TCR-CD3 assembly reactions were digested for 1 hour at 37°C with 500 U Endoglycosidase H (New England Biolabs, Beverly, MA), separated on 12% NuPAGE Bis-Tris gels (Invitrogen, Carlsbad, CA), transferred to PVDF membranes and exposed to phosphor imager plates. Gels were run under non-reducing conditions for all in vitro translation experiments shown, except for Fig. 5A, lower panel, which was run reducing. Densitometry was performed using the Wide Line Tool in the ImageQuant software package (Molecular Dynamics).

Supplemental References

Bartels, C., Xia, T., Billeter, M., Güntert, P., and Wüthrich, K. (1995). The program XEASY for computer-supported NMR spectral analysis of biological macromolecules. J Biomol NMR *6*, 1-10.

Call, M. E., Pyrdol, J., Wiedmann, M., and Wucherpfennig, K. W. (2002). The organizing principle in the formation of the T cell receptor-CD3 complex. Cell *111*, 967-979.

Chou, J. J., and Bax, A. (2001). Protein side-chain rotamers from dipolar couplings in a liquid crystalline phase. J Am Chem Soc *123*, 3844-3845.

Chou, J. J., Gaemers, S., Howder, B., Louis, J. M., and Bax, A. (2001). A simple apparatus for generating stretched polyacrylamide gels, yielding uniform alignment of proteins and detergent micelles. J Biomol NMR *21*, 377-382.

Chou, J. J., Li, S. P., and Bax, A. (2000). Study of conformational rearrangement and refinement of structural homology models by the use of heteronuclear dipolar couplings. Journal of Biomolecular NMR *18*, 217-227.

Cornilescu, G., Marquardt, J. L., Ottiger, M., and Bax, A. (1998). Validation of protein structure from anisotropic carbonyl chemical shifts in a dilute liquid crystalline phase. J Am Chem Soc *120*, 6836-6837.

Delaglio, F., Grzesiek, S., Vuister, G. W., Zhu, G., Pfeifer, J., and Bax, A. (1995). NMRPipe: a multidimensional spectral processing system based on UNIX pipes. J Biomol NMR *6*, 277-293.

Grzesiek, S., Vuister, G. W., and Bax, A. (1993). A Simple and Sensitive Experiment for Measurement of Jcc Couplings Between Backbone Carbonyl and Methyl Carbons in Isotopically Enriched Proteins. J Biomol NMR *3*, 487-493.

Hu, J. S., and Bax, A. (1996). Measurement of three-bond 13C-13C J couplings between carbonyl and carbonyl/carboxyl carbons in isotopically enriched proteins. J Am Chem Soc *118*, 8170-8171.

Hu, J.-S., Grzesiek, S., and Bax, A. (1997a). chi1 angle information from a simple two-dimensional NMR experiment which identifies trans 3JNCg couplings in isotopically enriched proteins. J Biomol NMR *9*, 323-328.

Hu, J.-S., Grzesiek, s., and Bax, A. (1997b). Two-dimensional NMR methods for determining c1 angles of aromatic residues in proteins from three-bond JC'Cg and JNCgcouplings. J Am Chem Soc *119*, 1803-1804.

Kay, L. E., Ikura, M., Tschudin, R., and Bax, A. (1990). Three-dimensional triple resonance NMR spectroscopy of isotopically enriched proteins. J Magn Reson *89*, 496-514.

Kuszewski, J., Gronenborn, A. M., and Clore, G. M. (1997). Improvements and extensions in the conformational database potential for the refinement of NMR and X-ray structures of proteins and nucleic acids. J Magn Reson *125*, 171-177.

Losonczi, J. A., Andrec, M., Fischer, M. W. F., and Prestegard, J. H. (1999). Order matrix analysis of residual dipolar couplings using singular value decomposition. J Magn Reson *138*, 334-342.

MacKenzie, K. R., Prestegard, J. H., and Engelman, D. M. (1996). Leucine side-chain rotamers in a glycophorin A transmembrane peptide as revealed by three-bond carbon-carbon couplings and 13C chemical shifts. J Biomol NMR *7*, 256-260.

Salzmann, M., Wider, G., Pervushin, K., and Wuthrich, K. (1999). Improved sensitivity and coherence selection for [15N,1H]-TROSY elements in triple resonance experiments. J Biomol NMR *15*, 181-184.

Sass, H. J., Musco, G., Stahl, S. J., Wingfield, P. T., and Grzesiek, S. (2000). Solution NMR of proteins within polyacrylamide gels: Diffusional properties and residual alignment by mechanical stress or embedding of oriented purple membranes. Journal of Biomolecular NMR *18*, 303-309.

Schwieters, C. D., Kuszewski, J. J., Tjandra, N., and Marius Clore, G. (2003). The Xplor-NIH NMR molecular structure determination package. J Magn Reson *160*, 65-73.

Szyperski, T., Neri, D., Leiting, B., Otting, G., and Wuthrich, K. (1992). Support of 1H NMR assignments in proteins by biosynthetically directed fractional 13C-labeling. J Biomol NMR *2*, 323-334.

Tycko, R., Blanco, F. J., and Ishii, Y. (2000). Alignment of biopolymers in strained gels: A new way to create detectable dipole-dipole couplings in high-resolution biomolecular NMR. J Am Chem Soc *122*, 9340-9341.

Vuister, G. W., Wang, A. C., and Bax, A. (1993). Measurement of three-bond nitrogen-carbon J couplings in proteins uniformly enriched in nitrogen-15 and carbon-13. J Am Chem Soc *115*, 5334-5335.

Walters, K. J., Matsuo, H., and Wagner, G. (1997). A Simple Method to Distinguish Intermonomer Nuclear Overhauser Effects in Homodimeric Proteins with C2 Symmetry. J Am Chem Soc *119*, 5958-5959.

Zweckstetter, M., and Bax, A. (2000). Prediction of sterically induced alignment in a dilute liquid crystalline phase: aid to protein structure determination by NMR. J Am Chem Soc *122*, 3791-3792.

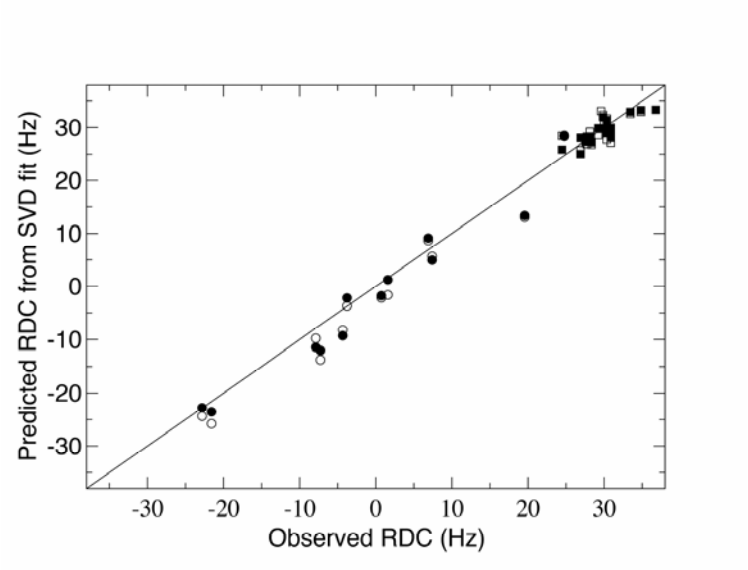

Figure S1. Singular Value Decomposition (SVD) Fit of All RDCs to the Representative Structure Determined from All Experimental Data

$^{1}D_{NH}$ and $^{1}D_{C\alpha H\alpha}$ couplings are shown as squares and circles, respectively. RDCs were simultaneously fit to all residues in the intact dimer with a Pearson correlation coefficient of 0.99 and a quality factor of 0.14. The results are grouped by monomer as indicated by either filled or unfilled symbols.

Table S1. Three-Bond *J* Couplings Used for Assigning Side-Chain χ_1 and χ_2 Rotamers

Residue	$^3J(NC\gamma)$ (Hz)	$^3J(C'C\gamma)$ (Hz)	$^3J(C\delta C\alpha)$ (Hz)	$\chi 1$ (degrees)	$\chi 2$ (degrees)
D(-3)					
S(-2)					
K(-1)	0.98			A	
L1-γ	1.71			180	
L1-δ1			2.35		A
L1-δ2			3.40		
C2					
Y3					
L4-γ	1.61			180	
L4-δ1			2.36		A
L4-δ2			3.22		
L5-γ	1.23			-60	
L5-δ1			2.82		A
L5-δ2			2.93		
D6		4.92		-60	
G7					
I8-γ2	2.03	1.54		-60	180
I8-δ1			3.57		
L9-γ	1.05				
L9-δ1			3.72		180
L9-δ2			0.78		
F10	2.52			180	
I11-γ2	1.93	1.03		-60	180
I11-δ1			3.61		
Y12	2.44			180	
G13					
V14-γ1	2.03	1.29		180	
V14-γ2	0.35	3.79			
I15-γ2	2.03	1.42		-60	180
I15-δ1			3.85		
L16-γ	1.27				
L16-δ1			1.57		-60
L16-δ2			2.88		
T17-γ2	2.19			180	
A18					
L19-γ	1.07			-60	

L19-δ1			3.83		180
L19-δ2			2.01		
F20	2.55			180	
L21-γ	0.88			-60	
L21-δ1			4.09		180
L21-δ2			1.58		
R22	1.70			180	
V23-γ1	1.52	1.66		180	
V23-γ2	0.82	2.72			
K24	1.62			180	
F25					
S26					
R27					
S28					
A29					
D30					

"A" indicates rotameric averaging for which no dihedral restraints were used during structure calculation. Rotamer information was extracted from the couplings according to analyses described in references (1–4).

1. Bax, A., Vuister, G. W., Grzesiek, S., Delaglio, F., Wang, A. C., Tschudin, R. & Zhu, G. (1994) *Methods Enzymol.* **239,** 79–105.

2. Chou, J. J., Case, D. & Bax, A. (2003) *J. Am. Chem. Soc.* **125,** 8959–8966.

3. MacKenzie, K. R., Prestegard, J. H. & Engelman, D. M. (1996) *J. Biomol. NMR* **7,** 256–260.

4. Hu, J. S., and Bax, A. (1996). *J. Am. Chem. Soc.* **118**, 8170-8171.